

# A study of the correlation length near a first-order phase transition : the three-dimensional three-state Potts model

Gvai, R. V.; Karsch, Frithjof; Petersson, Bengt

## **Suggested Citation**

Gvai, R. V. ; Karsch, Frithjof ; Petersson, Bengt (1989) A study of the correlation length near a first-order phase transition : the three-dimensional three-state Potts model. Nuclear Physics, B, 322(3), pp. 738-758

Posted at BiPrints Repository, Bielefeld University.

<http://repositories.ub.uni-bielefeld.de/biprints/volltexte/2009/3857>

# A STUDY OF THE CORRELATION LENGTH NEAR A FIRST-ORDER PHASE TRANSITION: THE THREE-DIMENSIONAL THREE-STATE POTTS MODEL

R.V. GAVAI\* and F. KARSCH

*Theory Division, CERN, CH-1211 Geneva 23, Switzerland*

B. PETERSSON

*Fakultät für Physik, Universität Bielefeld, Fed. Rep. Germany*

Received 28 December 1988  
(Revised 6 February 1989)

A high statistics study of the 3-d three-state Potts model on lattices of size  $L^3$ , with  $L$  ranging from 12 to 48, confirms the first-order nature of the  $Z(3)$  symmetry breaking phase transition in this model. We investigate the behaviour of spin–spin correlations in the critical region, comment on various methods to extract the correlation lengths and point out the resulting ambiguities on finite lattices. Our results indicate a finite correlation length at  $\beta_c$ . However, a careful analysis of the correlation functions is necessary to disentangle the inverse mass gap from the tunnelling correlation length which we found to diverge as  $L$  at  $\beta_c$  although the transition is clearly first order.

## 1. Introduction

With the advent of lattice gauge theories as a major tool to study non-perturbative aspects of quantum field theories, spin models, usually studied in the context of statistical mechanics, have increasingly become important for particle physics. In particular,  $Z(N)$  spin models play an important role in understanding the critical behaviour of  $SU(N)$  gauge theories at finite temperature. It has been argued that an effective theory for the order parameter of a  $(3 + 1)$ -dimensional gauge theory has the same global symmetry as the three-dimensional  $Z(N)$  spin models. Svetitsky and Yaffe [1] exploited the existing knowledge about  $Z(3)$  spin systems to predict a first-order phase transition for the physically interesting case of  $SU(3)$  gauge theory

\* On study leave from Tata Institute of Fundamental Research, Bombay 400005, India.

as no fixed point is known to exist for systems with global  $Z(3)$  symmetry. In addition, numerical studies of the three-dimensional three-state Potts model have indicated that it undergoes a first-order phase transition [2–4].

Early numerical studies of  $SU(3)$  gauge theory [5] on small lattices seemed to be in agreement with this prediction. They were later supported by studies on larger lattices [6, 7] which showed characteristic two-state signals and a shift of the critical coupling with increasing volume in accordance with the behaviour expected for a first-order phase transition [6]. Recently, however, a high-statistics computation of correlation lengths near the  $SU(3)$  phase transition has yielded a result which is strongly suggestive of a second-order phase transition [8]; the correlation length at  $T_c$  increases with the size of the system. A concurrent study [9] of the order parameter and energy density, on the other hand, suggested a first-order phase transition although weaker than previously thought. As in ref. [5], clear metastabilities were found in this study of the order parameter on the largest spatial lattice analyzed so far.

If further studies on larger spatial lattices confirm the conclusions of ref. [8], then a fresh look at the universality argument may be needed. On the other hand the phase transition in the 3-d three-state Potts model is also known to be rather weak; the numerical studies which lead to the conclusion of a first-order phase transition in this model were based on moderate statistics by today's standards. Moreover, only global observables were studied in those investigations and very little is known about the behaviour of the correlation lengths for the 3-d Potts model [4, 10]. It should be noted that the different conclusions of refs. [8] and [9] stem from the analysis of different physical observables. It is not clear which observable is a better one to study the order of the phase transition if it were to be a weak first-order transition. It may well be that an analysis of bulk quantities, as they have been studied in ref. [9], are more efficient in this case than the correlation length studied in ref. [8]. In view of all this we studied both the correlation length and bulk quantities in a high-statistics investigation of the Potts model on lattices of various sizes ranging from  $12^3$  up to  $48^3$ . Our analysis of global observables like the order parameter confirms the first-order nature of the phase transition in the 3-d three-state Potts model. The analysis of the correlation lengths appears, however, to be more subtle and less conclusive since the determination of the physical mass gap on a finite lattice is difficult due to the presence of a large tunnelling correlation length in the critical region. We find that reasonable estimates of the mass gap at  $\beta_c$  are almost independent of  $L$  and yield a correlation length  $\xi \sim 10$ .

The plan of our paper is the following. In the next section we describe the Potts model and present our results on the phase structure obtained from global observables. In sect. 3 we analyze spin–spin correlation functions and obtain correlation lengths using various methods. Finally we present our conclusions in sect. 4 and discuss the relevance of our findings to the phase transitions in the  $SU(3)$  gauge theory.

## 2. The phase structure of the Potts model

The 3-d three-state Potts model is defined by the hamiltonian

$$H = -\frac{3}{2}\beta \sum_{\langle j, k \rangle} \delta_{\sigma_j, \sigma_k} = -\beta \sum_{\langle j, k \rangle} [s_j \cdot s_k^\dagger + s_j^\dagger \cdot s_k + \text{const.}], \quad (2.1)$$

where the sum is over nearest-neighbour pairs  $\langle j, k \rangle$  and  $\sigma_{j(k)} = 0, 1$  or  $2$ . The second equality in eq. (2.1) exploits the fact that the three-state Potts model is equivalent to the  $Z(3)$  spin model with spins  $s_j = \exp(2\pi i \sigma_j/3)$ . The partition function of the system on an  $L^3$  cubic lattice is given by

$$Z = \sum_{\{\sigma_j\}} e^{-H}. \quad (2.2)$$

For ferromagnetic ( $\beta > 0$ ) coupling the above model is known to undergo a phase transition from a  $Z(3)$  symmetric phase for  $\beta < \beta_c$  to a spontaneously broken phase for  $\beta > \beta_c$  at a critical coupling  $\beta_c \approx 0.367$  [4]. Renormalization group studies [2] and Monte Carlo simulations [3] suggest the transition to be weakly first order. No systematic finite size study of the model has been performed so far. In the following we will study the volume dependence of global observables like the average action

$$E = \left\langle \frac{1}{3L^3} \sum_{\langle j, k \rangle} \cos\left(\frac{2\pi}{3}(\sigma_j - \sigma_k)\right) \right\rangle, \quad (2.3)$$

and the order parameter

$$S = \langle \max(S_0, S_1, S_2) \rangle, \quad (2.4)$$

with  $S_\alpha$  defined by

$$S_\alpha = \text{Re} \left( \frac{e^{2\pi i \alpha/3}}{L^3} \sum_j s_j \right), \quad \alpha = 0, 1, 2. \quad (2.5)$$

Here  $\langle X \rangle$  denotes the thermal expectation value of the observable  $X$  with respect to  $Z$ . We used the standard Metropolis algorithm to simulate the model on periodic cubic lattices of sizes  $L = 12, 20, 24, 30, 36$  and  $48$ . Typically we performed  $5 \times 10^5 - 5 \times 10^6$  iterations at each  $\beta$  value. Expectation values were computed every 10th iteration. To eliminate the remaining time correlations errors have been calculated by dividing the data sample into blocks of various lengths and taking the expectation values on a given block as independent measurements. Figs. 1 and 2 show results for  $S$  and  $E$  as a function of  $\beta$ . One sees from these figures that the cross-over in the critical region becomes sharper with increasing volume. They, therefore, suggest that a discontinuity will develop in both observables in the

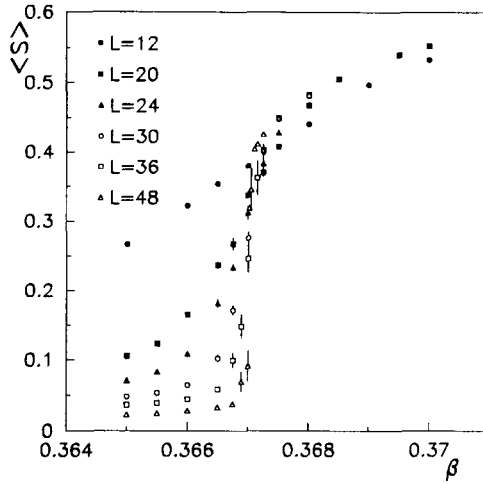


Fig. 1. The order parameter  $S$  versus  $\beta$  on lattices of size  $L^3$  with  $L = 12, 20, 24, 30, 36$  and  $48$ .

infinite volume limit. This is further supported by the behaviour of the inverse function  $\beta(L, E)$ , i.e. the coupling  $\beta$  at which the action takes on the value  $E$  on a lattice of size  $L^3$ . Fig. 3 displays  $\beta(L, E)$  for three values of  $E$  as a function of  $L$ . The points shown have been obtained from a cubic spline fit to the data of fig. 2. On the  $48^3$  lattice our statistics in the critical region were insufficient and we simply used a straight line interpolation. The lines drawn are extrapolations of the results

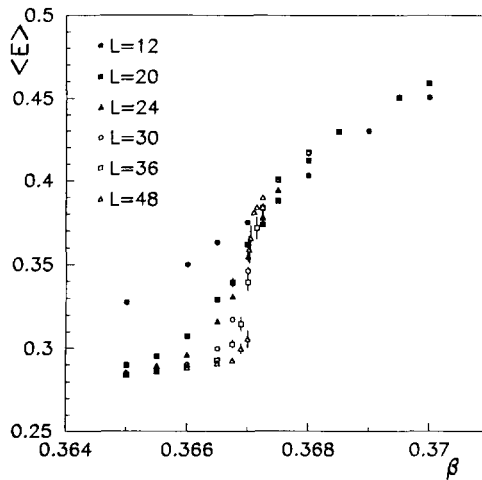


Fig. 2. Same as fig. 1 but for the average action  $E$ .

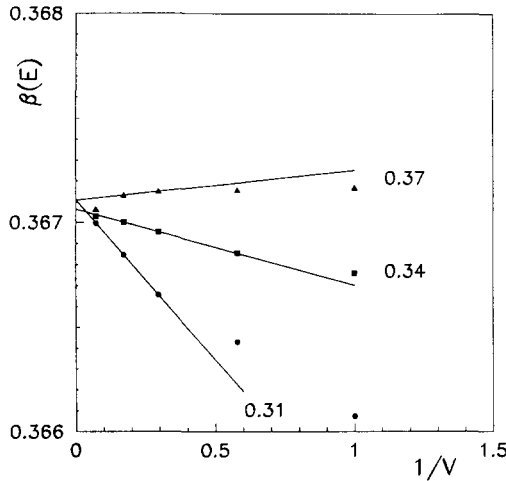


Fig. 3. The inverse function  $\beta(L, E)$  versus  $1/V$  for the values of  $E$  indicated on the figure. The volume  $V$  is measured in units of  $20^3$ . The straight lines shown are extrapolations of the data for  $L = 30$  and  $36$ .

obtained for  $L = 30$  and  $36$ . They strongly suggest that  $\beta(L, E)$  indeed becomes multi-valued at  $\beta_c$ ,

$$\forall E_{\min} \leq E \leq E_{\max}, \quad \lim_{L \rightarrow \infty} \beta(L, E) = \beta_c. \quad (2.6)$$

In order to see what causes the rapid change in both the observables in the critical region we looked at the evolution of the order parameter as a function of Monte Carlo time and its probability distribution. Figs. 4 and 5 show the time evolution of  $S$  for  $\beta$  close to  $\beta_c$  on  $36^3$  and  $48^3$  lattices, respectively. On both lattices one sees clear flip-flops between two well-separated states. This is reflected in the clearly separated peaks of the probability distributions, shown in fig. 6, corresponding to a globally  $Z(3)$  symmetric and a spontaneously broken phase. There are no indications that the peaks approach each other as the lattice size increases. Furthermore the number of flips from one phase to another decreases rapidly with increasing volume and the overlap of the two peaks in the probability distribution function reduces simultaneously.

The clear separation between the two phases in the critical region suggests separating the data and averaging them in the respective phases. This is shown in fig. 7 for the order parameter and the action. We note that the discontinuity in the order parameter increases with increasing volume and that the region of coexisting states shrinks at the same time. In fact, on the  $48^3$  lattice the metastability region was as small as  $3 \times 10^{-5}$ . For the gap in  $S$  and  $E$  we extract from our data

$$\Delta S = 0.395 \pm 0.005, \quad \Delta E = 0.080 \pm 0.004, \quad (2.7)$$

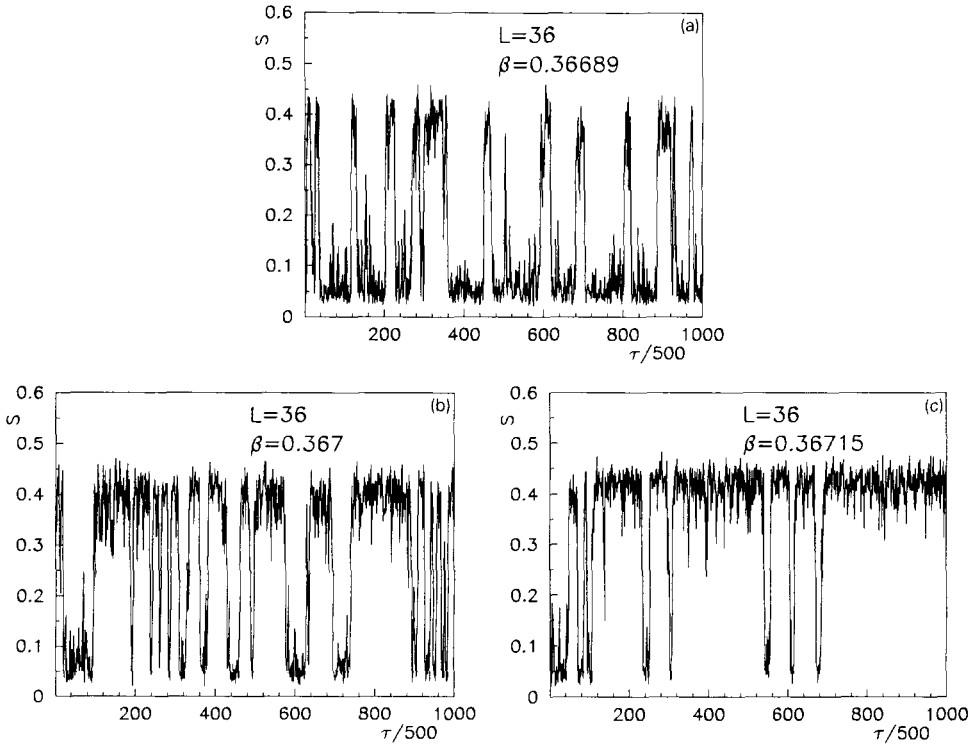


Fig. 4. (a-c) Time history of the order parameter  $S$  as a function of Monte Carlo time on the  $L = 36$  lattice close to the critical coupling for that lattice.

with  $E_{\min}(\beta_c) = 0.297 \pm 0.002$  and  $E_{\max}(\beta_c) = 0.377 \pm 0.002$ . We note that the gap in the order parameter is quite large (40% of the maximal value). The weakness of the transition results from the large slope of the action at  $\beta_c$ .

The scaling behaviour of a statistical system near a phase transition is characterized by its critical exponents. Phase transitions in spin models can be classified by the thermal and magnetic exponents  $y_T$  and  $y_H$  that control the critical behaviour near the fixed point. The scaling of the critical coupling  $\beta_{c,L}$  as well as the width of the critical region,  $\sigma_L$ , is expected [10] to be governed by the thermal exponent  $y_T = 1/\nu = d/(2 - \alpha)$

$$\beta_{c,L} - \beta_c \sim L^{-y_T}, \quad \sigma_L \sim L^{-y_T}. \tag{2.8}$$

For a first-order phase transition governed by a discontinuity fixed point\*  $y_T$  is

\*In general, the predictions about the critical behaviour near a first-order phase transition rely on the existence of a discontinuity fixed point. There are indications from Monte Carlo renormalization group studies [2] that the 3-d three-state Potts model might not have such a fixed point. For a discussion of the scaling behaviour independent of the existence of discontinuity fixed point, see ref. [11].

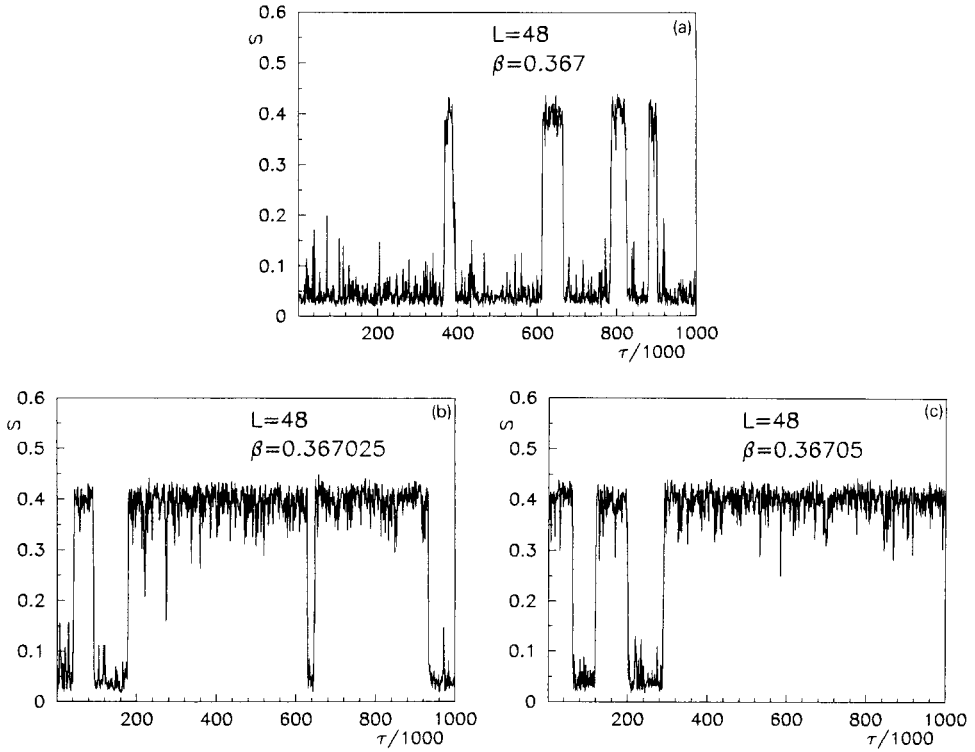


Fig. 5. (a-c) Same as fig. 3 but for  $L = 48$  lattice.

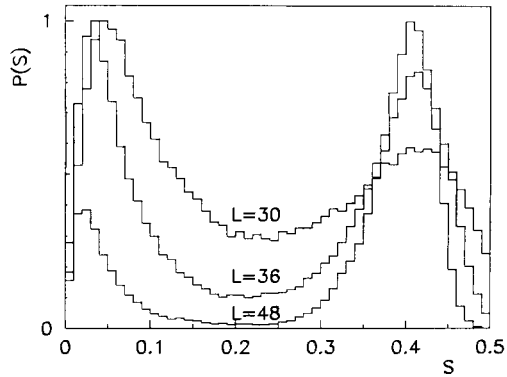


Fig. 6. Probability distribution of the order parameter  $S$  for (a)  $L = 30$  at  $\beta = 0.36675$ , (b)  $L = 36$  at  $\beta = 0.367$  and (c)  $L = 48$  at  $\beta = 0.367025$ .



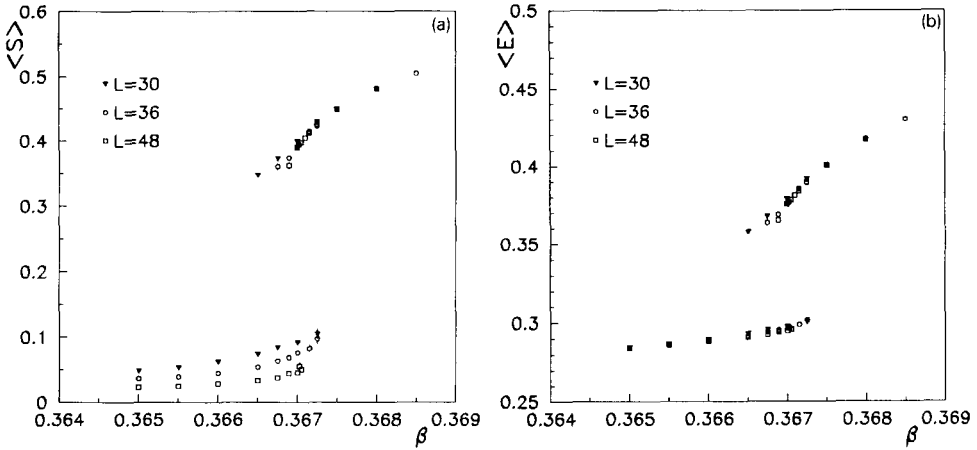


Fig. 7. (a) The order parameter and (b) the average action in the critical region as a function of  $\beta$  on  $30^3$ ,  $36^3$  and  $48^3$  lattices.

simply given by  $d$ . In this case  $\beta_{c,L}$  and  $\sigma_L$  are thus expected to scale with the volume of the system, whereas a slower approach to the asymptotic values is expected for a second-order transition ( $\alpha < 1$ ). It is therefore worthwhile to investigate the volume dependence of  $\beta_{c,L}$  and  $\sigma_L$  and determine  $y_T$  in our case.

In order to define both  $\beta_{c,L}$  and  $\sigma_L$  we exploited the metastable behaviour of the system in the critical region, where one observes several flips between the symmetric and broken phase. For instance, on the  $36^3$  lattice we counted 65 flips at  $\beta = 0.367$  in  $10^6$  iterations (the first half of this run is shown in fig. 4b). The relative population of the different phases thus is statistically significant. We, therefore, defined the critical coupling,  $\beta_{c,L}$ , and the width of the metastable region,  $\sigma_L$  on a lattice of volume  $V = L^3$  by determining the point where the order parameter spent equal time in both phases. As a criterium to define the population of the two phases,  $P_{1,(2)}(\beta, L)$ , we used the minimum of the probability distribution,  $P(\beta, L)$ , between the two peaks to separate the phases and counted the number of events under the respective peaks which are clearly evident in fig. 6. The relative population density is then defined by

$$\Delta P(\beta, L) = 1 - |P_1 - P_2| / (P_1 + P_2). \tag{2.9}$$

We performed a gaussian fit to the relative population density,

$$\Delta P(\beta, L) = \exp \left[ -\frac{1}{2} \left( \frac{\beta - \beta_{c,L}}{\sigma_L} \right)^2 \right], \tag{2.10}$$

TABLE 1  
The critical couplings and the width of the metastability region on various lattices as obtained from a gaussian fit to the relative population density of the broken and symmetric phases

$L$	$\beta_{c,L}$	$\sigma_L \times 10^4$
20	0.36649(1)	6.69(5)
24	0.36670(1)	3.98(8)
30	0.36691(1)	1.93(6)
36	0.36699(1)	1.30(8)
48	0.367025(25)	0.25

to obtain  $\beta_{c,L}$  and  $\sigma_L$ . The results of the fits are given in table 1, where  $\beta_c$  and  $\sigma_L$  are the peak and the width of the gaussian, respectively. Since on the  $48^3$  lattice only a few flips occurred even in runs of  $10^6$  iterations, as shown in fig. 5, we adopted a different procedure for it. Flips have been observed only in the interval  $0.367 \leq \beta \leq 0.36705$ . The length of this interval was taken to be  $\sigma_{48}$  and the midpoint of the interval was taken as  $\beta_{c,48}$ . For lattices of size  $24^3$  and larger the shifts in  $\beta_{c,L}$  and  $\sigma_L$  are both consistent with a  $1/V$  behaviour, as displayed in fig. 8. Linear fits of the forms

$$\beta_{c,L} = \beta_{c,\infty} - A/L^3, \quad (2.11a)$$

and

$$\sigma_L = B/L^3 \quad (2.11b)$$

yield  $\beta_{c,\infty} = 0.36708(2)$ ,  $A = 4.9(2)$ ,  $B = 5.37(8)$ . We also checked that assuming the more general form, given by eq. (2.9), yields a value of  $y_T$  consistent with three.

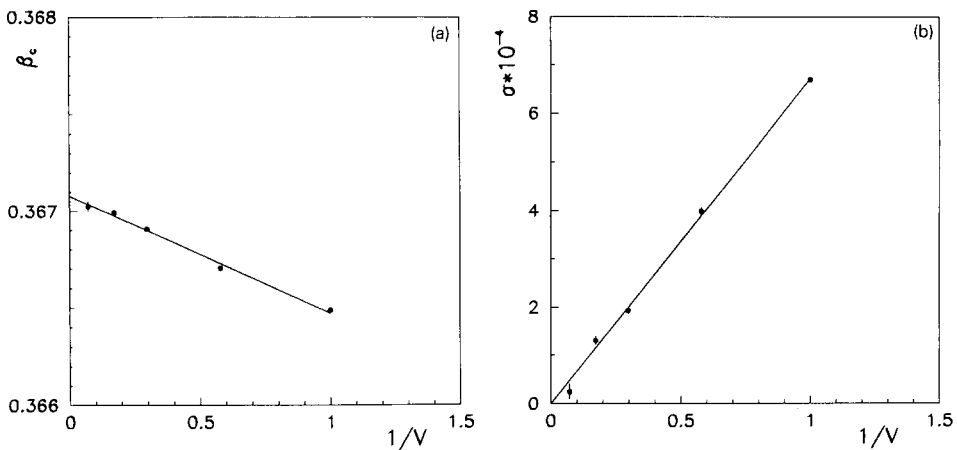


Fig. 8. Finite size scaling of (a)  $\beta_{c,L}$  and (b)  $\sigma_L$ . The volume  $V$  is measured in units of  $20^3$ .

Both of these findings are in accord with the expectation that the phase transition is first order.

Let us summarize the main findings of this section that re-establish the first-order nature of the phase transition in the ferromagnetic 3-d three-state Potts model:

(i) Physical quantities such as the order parameter exhibit distinct metastable behaviour in the critical region.

(ii) The probability distribution functions show a clear two-peak structure. With increasing volume the peaks become sharper and move a little away from each other, if at all.

(iii) The difference  $\beta_c - \beta_{c,L}$  as well as the width of the metastable region,  $\sigma_L$ , scales with  $1/V$ .

(iv) The inverse function  $\beta(L, E)$ , where  $E$  is the action, appears to become multi-valued for  $0.297 \leq E \leq 0.377$  in the infinite volume limit at  $\beta_c = 0.36708$  which is in agreement with the  $\beta_c$  obtained by demanding equal population in the two phases.

### 3. Correlation lengths on finite lattices

#### 3.1. PRELIMINARIES

Having re-established that the 3-d three-state Potts model has a first order phase transition [2, 3], we present here the results of our investigation of the correlation lengths of the system close to the critical point. As mentioned earlier, such a study of the correlation length in SU(3) pure gauge theory at finite temperature gave rise to a controversy about the order of the deconfinement phase transition. Based on studies similar to those in sect. 2 a first-order deconfinement phase transition was found in SU(3), whereas a study of correlation lengths alone suggested a second-order transition.

In order to study the correlation length one analyses the corresponding correlation functions. The spin-spin correlation functions that we study are defined by

$$\Gamma_1(r) = (1/6V) \left\langle \sum_i s_i s_j^\dagger \right\rangle, \tag{3.1}$$

and the corresponding zero-momentum projection given by

$$\Gamma_0(r) = (1/6L) \left\langle \sum_{i=1}^L \bar{s}_i \bar{s}_j^\dagger \right\rangle. \tag{3.2}$$

Here  $s_i$  denotes the spin at site  $i$ .  $\bar{s}_i$  is the average spin on the plane  $i$ , and  $r = |i - j|$  denotes the distance between the sites (planes)  $i$  and  $j$  along one of the principal

axes of the lattice. The connected part of these correlation functions,

$$\Gamma_{i,c}(r) = \Gamma_i(r) - \lim_{r \rightarrow \infty} \Gamma_i(r), \quad (3.3)$$

decays exponentially at large distances. The correlation length can be obtained from it as

$$\xi^{-1} = - \lim_{r \rightarrow \infty} \frac{1}{r} \ln \Gamma_{i,c}(r). \quad (3.4)$$

In a finite volume (as well as in any numerical simulation) the large distance behaviour of the correlation function is not accessible to us. Even on rather large lattices the subleading powerlike behaviour of the correlation function can be non-negligible. Thus unlike the global quantities studied in the previous section extraction of the correlation length,  $\xi$ , on these lattices is not totally unambiguous. In general, it requires an assumption on the functional form of  $\Gamma_i(r)$ . A popular procedure is to form ratios of the correlation functions, like

$$R_i^\alpha(r) = \Gamma_i(r) / (\Gamma_i(r+1)). \quad (3.5)$$

Using an ansatz inspired by the behaviour of  $\Gamma$  on an infinite lattice that takes into account the periodicity of the  $L^3$  lattice

$$\Gamma_i(r) = A_i \left( \exp(-r/\xi) / r^i + \exp(-(L-r)/\xi) / (L-r)^i \right) \quad (3.6)$$

with  $i = 0, 1$ , one can then extract a correlation length  $\xi$ . The ratios  $R_i^\alpha$  are sensitive to the behaviour of the correlation functions near  $r$ . From them one can define respective distance-dependent masses,  $m_i^\alpha(r) = 1/\xi_i^\alpha(r)$ , as solutions of eq. (3.5) using the ansatz given in eq. (3.6). The large distance behaviour of these estimators yields  $\xi^{-1}$ , if the distance-dependent masses exhibit a plateau at large distances. However, a technical remark about this ansatz may be in order.

In eq. (3.6) the periodicity in the longitudinal direction has been taken into account by explicitly adding the contribution of the closest image of the source in that direction. In principle, further away images in longitudinal as well as transverse directions also contribute. In fact, their contribution becomes more significant as  $\xi$  increases and an increasing number of images has to be included in eq. (3.6) to get agreement with masses extracted from  $\Gamma_0$  and  $\Gamma_1$ , respectively. We therefore replaced in our analysis the ansatz for  $\Gamma_1(r)$  by a generalized periodic exponential

$$\Gamma_1(r) = A \sum_{m=-\infty}^{\infty} \sum_{j=-\infty}^{\infty} \sum_{k=-\infty}^{\infty} \frac{1}{\left[ (r/L + m)^2 + j^2 + k^2 \right]^{1/2}} \times \exp \left[ (-L/\xi) \sqrt{(r/L + m)^2 + j^2 + k^2} \right]. \quad (3.7)$$

Note that the contribution of the images need not be added explicitly to  $\Gamma_0(r)$ , since the corresponding expression for it can be summed up exactly and one again obtains the same form as in eq. (3.6) with just a renormalization of  $A_0$ .

We find that  $m_0^\alpha(r)$  and  $m_1^\alpha(r)$  obtained by using eq. (3.7) always coincide, whereas the corresponding masses extracted by using eq. (3.6) differ by an increasing amount as the mass becomes smaller. For  $m_0^\alpha \sim 0.05$  the discrepancy is as much as 100%. This is also true if one fits the correlation function data to the forms given by eqs. (3.6) and (3.7) in order to extract the correlation lengths instead of using the distance-dependent masses. As is well known, the fits exploit the information at all  $r$  while the distance-dependent masses are more local.

### 3.2. NUMERICAL ANALYSIS OF $R^\alpha$

We begin the discussion of our numerical results by first demonstrating that the estimates for  $m_i^\alpha(r)$  indeed coincide for  $i = 0$  and 1. Fig. 9 displays these quantities on the  $36^3$  lattice for a large range of  $\beta$  that includes the critical region. From the analysis of the previous section we know that on the  $36^3$  lattice the phase transition occurs at  $\beta_{c,36} = 0.36699$  with a metastable region of characteristic size  $O(\sigma = 0.0001)$ . Although the asymptotic value of the distance-dependent masses changes very rapidly in this region we note that no significant change occurs in the functional behaviour, i.e. they all are essentially flat over a large range of  $r$ . This seems to indicate that eq. (3.7) provides already a good description of the data; any contributions from higher excited states have either a large mass and/or a small amplitude. Furthermore, we also note that any addition of a constant to eq. (3.7)

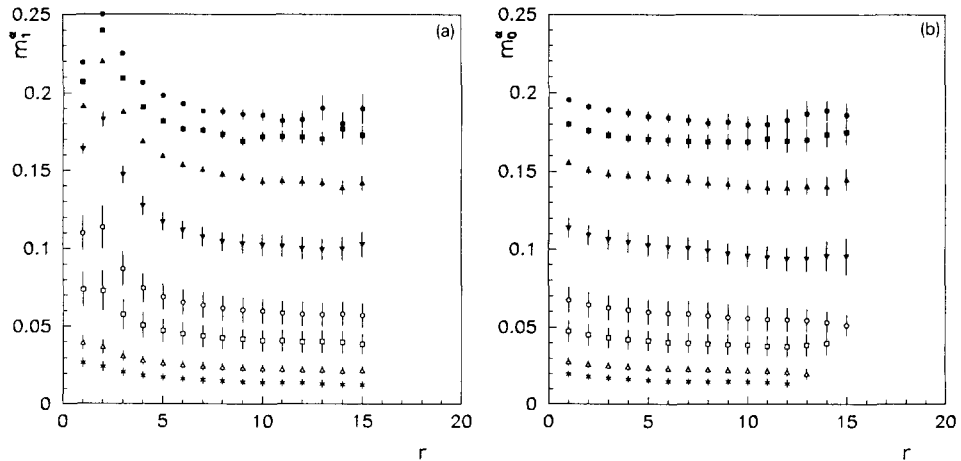


Fig. 9. The distance-dependent masses (a)  $m_1$  and (b)  $m_0$  as a function of  $r$  for the ratio  $R^\alpha$  on  $36^3$  lattice. Starting from the top the  $\beta$  values are 0.365, 0.3655, 0.366, 0.3665, 0.36675, 0.36689, 0.367 and 0.36715.

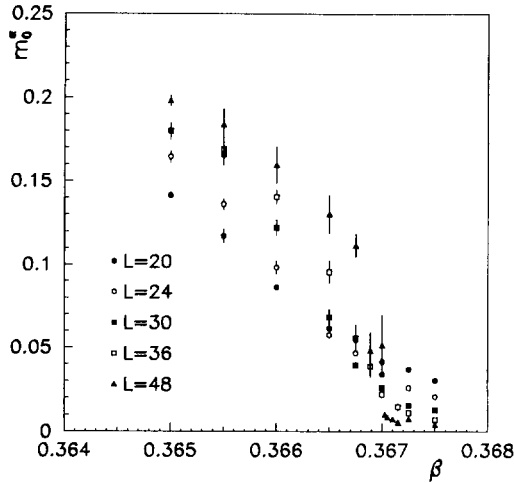


Fig. 10.  $m_0^\alpha$  as a function of  $\beta$  for  $L^3$  lattices with  $L = 20, 24, 30, 36$  and  $48$ .

does not appear to be necessary. In view of the good agreement between  $m_0$  and  $m_1$ , obtained by using eq. (3.7), we will display the results for any one of them only in the following.

In fig. 10 we show  $m_0^\alpha$  for all  $\beta$  values studied by us on lattices of size  $L = 20$  up to  $L = 48$ . The estimates of  $m_0^\alpha$  are based on distance-dependent masses taken at  $r = 7$  for  $L = 20, 24$  and  $r = 10$  for  $L = 30, 36$  and  $48$ . We have checked that  $m_0^\alpha(r)$  develops a plateau at this distance (see fig. 9 for  $L = 36$ ) and also verified that a fit to the correlation functions gave masses in agreement with those shown in fig. 10. Results obtained from  $m_0^\alpha(r)$  and the fits for all lattices we studied are summarized in tables 2 and 3. They show that  $m_0^\alpha$  decreases with increasing lattice size for large  $\beta$ , whereas it shows the opposite trend for small  $\beta$ . We note that at  $\beta = 0.367$ ,  $m_0^\alpha$  decreases for  $20 \leq L \leq 36$  and is consistent with a  $1/L$  behaviour. In fact we find

$$m_0^\alpha \simeq 0.8/L \quad \text{for } L \leq 36, \quad \beta = 0.367. \quad (3.8)$$

As shown in table 4, this trend only stops on the  $48^3$  lattice where we find  $m_0 = 0.0744$ . This is as expected: For all lattices  $L = 20$  up to  $L = 36$  we observe a large number of tunnellings between the symmetric and broken phase at  $\beta = 0.367$ . The potential barrier between these two phases increases with increasing lattice size (see fig. 6) and the tunnelling probability thus decreases. This leads to an increase in the tunnelling correlation length with increasing lattice size. On the  $48^3$  lattice, however, the critical coupling shifts to a slightly higher value ( $\beta_{c,48} = 0.367025$ ) and the coupling  $\beta = 0.367$  moves to the edge of the metastability region, i.e. we see no significant contribution from tunnellings to the broken phase. This leads to the smaller correlation length on the  $48^3$  lattice at  $\beta = 0.367$ . In fact, when we move

TABLE 2  
 $m_0^\alpha$  for all values of  $\beta$  and lattices of sizes  $L = 20, 24, 30, 36$  and  $48$  obtained from distance-dependent masses  $m_0^\alpha(7)$  for  $L = 20$  and  $24$  and  $m_0^\alpha(10)$  for  $L = 30, 36,$  and  $48$

$L \backslash \beta$	20	24	30	36	48
0.365	0.141(2)	0.164(3)	0.180(3)	0.180(5)	0.198(3)
0.3655	0.117(4)	0.136(3)	0.166(6)	0.169(5)	0.184(9)
0.366	0.086(1)	0.098(4)	0.122(5)	0.141(4)	0.160(11)
0.3665	0.061(2)	0.058(2)	0.068(5)	0.096(7)	0.130(11)
0.36675	0.055(2)	0.047(1)	0.040(2)	0.056(8)	0.112(7)
0.36689	—	—	—	0.039(7)	0.048(11)
0.367	0.041(2)	0.034(1)	0.026(1)	0.022(2)	0.051(18)
0.367025	—	—	—	—	0.010(2)
0.36705	—	—	—	—	0.008(1)
0.3671	—	—	—	—	0.007(1)
0.36715	—	—	—	0.015(2)	0.005(1)
0.36725	0.037(1)	0.026(1)	0.016(1)	0.011(1)	0.008(1)
0.3675	0.030(1)	0.021(1)	0.013(1)	0.007(1)	0.004(1)
0.368	0.023(2)	—	0.009(1)	0.006(1)	0.004(1)

TABLE 3  
 $m_0^\alpha$  for all values of  $\beta$  and lattices of sizes  $L = 20, 24, 30, 36$  and  $48$  obtained from fits to the correlation functions  $F_0(r)$ . Fits for  $L \geq 24$  have been performed for  $r \geq 6$ , while those for  $L = 20$  are based on all  $r \geq 4$ .

$L \backslash \beta$	20	24	30	36	48
0.365	0.142(5)	0.164(5)	0.181(2)	0.182(2)	0.201(1)
0.3655	0.118(14)	0.136(5)	0.162(5)	0.168(3)	0.182(5)
0.366	0.087(9)	0.098(10)	0.121(7)	0.141(3)	0.156(4)
0.3665	0.062(17)	0.058(12)	0.066(19)	0.089(12)	0.122(6)
0.36675	0.055(23)	0.047(9)	0.040(15)	0.046(23)	0.109(4)
0.36689	—	—	—	0.032(25)	0.036(23)
0.367	0.042(14)	0.034(15)	0.026(14)	0.021(21)	0.027(27)
0.367025	—	—	—	—	0.009(18)
0.36705	—	—	—	—	0.008(15)
0.3671	—	—	—	—	0.007(3)
0.36715	—	—	—	0.014(21)	0.007(2)
0.36725	0.038(14)	0.026(13)	0.016(15)	0.011(9)	0.006(3)
0.3675	0.032(12)	0.022(7)	0.013(5)	0.008(3)	0.004(1)
0.368	0.025(3)	—	0.010(2)	0.006(2)	0.003(2)

TABLE 4  
Scaling of  $m_0^\alpha$  with  $L$  at  $\beta = 0.367$

$L$	$m_0^\alpha$	$m_0^\alpha L$
20	0.0414(9)	0.828(30)
24	0.0340(10)	0.814(24)
30	0.0259(8)	0.777(24)
36	0.0221(21)	0.796(76)
48	0.0514(181)	2.47(87)

close to the critical point of the  $48^3$  lattice,  $\beta = 0.367025$ , we find an increasing correlation length for all our lattices up to  $L = 48$ . The increase of  $\xi$  is again consistent with  $\xi \sim L$ .

The behaviour of  $\xi$  discussed above is consistent with that expected for a second-order phase transition. However, it need not contradict our conclusions of sect. 2. Also for a first-order phase transition the correlation length diverges at  $\beta_c$  [12, 13] if the infinite volume limit is taken at fixed  $\beta = \beta_c$ :

$$\lim_{L \rightarrow \infty} \lim_{\beta \rightarrow \beta_c^-} \xi(\beta, L) = \lim_{L \rightarrow \infty} \xi(\beta_c, L) \rightarrow \infty. \quad (3.9)$$

For a strong first-order transition this divergence is in general expected to be faster than  $L$  [12]. However, a slow rise consistent with  $\xi \sim L$  is possible for a weak first-order transition. Note that the conventional wisdom of a finite correlation length for a first-order transition corresponds to the interchange of the two limits in eq. (3.9), i.e., the thermodynamic limit is taken first. A similar behaviour is known to occur for other related quantities such as the specific heat and the magnetic susceptibility of systems with first-order phase transitions [10, 12]; they all develop  $\delta$ -function like singularities at  $\beta_c$  if the limits are taken as in eq. (3.9) and stay finite otherwise. Unfortunately, the nonmonotonic nature of our data close to  $\beta_c$ , shown in fig. 10, does not allow us to distinguish between the two limits clearly.

It may be worth emphasizing here that our analysis of  $R^\alpha$  to extract the mass  $m^\alpha$  is very similar to the one performed for the SU(3) gauge theory in ref. [8]. The same observables were used in both the cases and the behaviour found at  $\beta_c$  seems to be identical for the SU(3) gauge theory and the 3-d three-state Potts model. However, contrary to what has been claimed in ref. [8] we do not see any indication for a qualitative change in the distance-dependent masses at  $\beta_c$  that would justify the subtraction of a constant from the correlation functions in the broken phase.

### 3.3. TUNNELLING CORRELATION LENGTH AND THE PHYSICAL MASS GAP

The large correlation length found above  $\beta_c$  is clearly not of physical relevance. In fact, it is a genuine finite size effect related to the tunnelling between degenerate



vacua [13–16]. From an analysis of the transfer matrix one expects in general the correlation function to be a coherent sum of its eigenvalues. For instance, considering only the contribution of the two smallest eigenvalues above the ground state the correlation functions  $\Gamma_0$  is expected to be described by

$$\Gamma_0(r) \sim A e^{-r/\xi_G} + B e^{-r/\xi_T}. \tag{3.10}$$

The correlation lengths entering the two leading terms can in general be related to the inverse mass gap,  $\xi_G = 1/m_G$ , and the tunnelling correlation length,  $\xi_T$ . In the spectrum of the transfer matrix the latter arises from the level splitting associated with the tunnelling between different degenerate vacua. In the infinite volume limit the barrier between these vacua becomes infinitely large, causing  $\xi_T \rightarrow \infty$  in the broken phase. This gives rise to the usual constant disconnected part in the correlation function. In the symmetric phase one expects  $\xi_T \sim \xi_G$  for  $L \rightarrow \infty$ . The above scenario for the tunnelling correlation length can be explicitly verified in exactly solvable two-dimensional Ising model [17] as well as in numerical simulations of higher dimensional models [18].

The correlation length obtained from the ratios  $R^\alpha$  behaves in a manner consistent with what one expects for the tunnelling correlation length for  $\beta \geq \beta_c$ . One thus has to be careful in interpreting the results for  $\xi$  close to  $\beta = 0.367025$ . It appears reasonable to expect that the correlation lengths  $\xi_G$  and  $\xi_T$  get intertwined in the critical region and the estimate from  $R_i^\alpha$  corresponds to neither of them alone. One way to eliminate  $\xi_T$ , if it is large enough, is to define [19] the ratios

$$R_i^\beta(r) = \frac{\Gamma_i^{\text{diff}}(r, r+1)}{\Gamma_i^{\text{diff}}(r+1, r+2)}, \tag{3.11}$$

and obtain the distance-dependent masses from them. Here  $\Gamma_i^{\text{diff}}(r_1, r_2)$  is defined through

$$\Gamma_i^{\text{diff}}(r_1, r_2) = \Gamma_i(r_1) - \Gamma_i(r_2). \tag{3.12}$$

For  $r_2 \rightarrow \infty$  this coincides with the usual definition of connected correlation functions on infinite lattices. Note that the ratios  $R_i^\alpha$  and  $R_i^\beta$  yield the same mass at any distance, if the correlation functions are indeed given by a single exponential. If, on the other hand, they are given by a superposition of two or more exponentials as in eq. (3.9), then  $\Gamma^{\text{diff}}(r, r+1)$  yields a superposition of the same exponentials but with a new ordering of their relative weights. In fact, for the form given by eq. (3.9) one has

$$\Gamma_0^{\text{diff}}(r, r+1) \sim \tilde{A} e^{-r/\xi_G} + \tilde{B} e^{-r/\xi_T}, \tag{3.13}$$

with

$$\frac{\tilde{B}}{\tilde{A}} = \frac{(1 - e^{-1/\xi_T})B}{(1 - e^{-1/\xi_G})A}. \quad (3.14)$$

The relative weight of the contribution coming from a tunnelling correlation length thus goes to zero for  $\xi_T \rightarrow \infty$ .  $\Gamma^{\text{diff}}$  thus is expected to be dominated again by a single exponential, which, however, now decays according to the next leading correlation length.

A comparison of distance-dependent masses based on  $R_0^\alpha$  and  $R_0^\beta$  is shown in fig. 11 for  $\beta = 0.365$  and  $\beta = 0.367$ . It may be noted that the masses  $m_0^\beta(r)$ , obtained from the ratios  $R_0^\beta(r)$  by using eq. (3.6), show a stronger  $r$  dependence. They reach a plateau for  $r \geq 5$  whereas  $m_0^\alpha(r)$  is essentially  $r$  independent for  $r \geq 2$ , suggesting the presence of more than one relevant mass scale. This is much more pronounced in the critical region. Despite the large errors on  $m_0^\beta$ , which are due to the difference of the correlation functions in  $\Gamma_0^{\text{diff}}$ , one sees that both procedures agree in the symmetric phase, while they lead to very different results in the critical region. Results of fits to  $\Gamma_1^{\text{diff}}(r, r+1)$  using the periodic exponential defined in eq. (3.7) for  $\Gamma_1$  are given in table 5. We have also analysed the distance-dependent masses obtained from  $R_i^\beta$ . In general, they are in agreement with the results in table 5.

A comparison of the results in tables 2 and 3 with those in table 5 shows that  $m^\alpha \sim m^\beta$  for  $\beta \leq 0.36675$  for our largest lattice. However, we find that  $m^\beta$  reaches a minimum at  $\beta = \beta_{c,L}$ , unlike the masses  $m^\alpha$ , and increases again in the broken phase. Indeed, as  $m^\alpha \leq 0.05$  in this region, one sees from eq. (3.14), that the

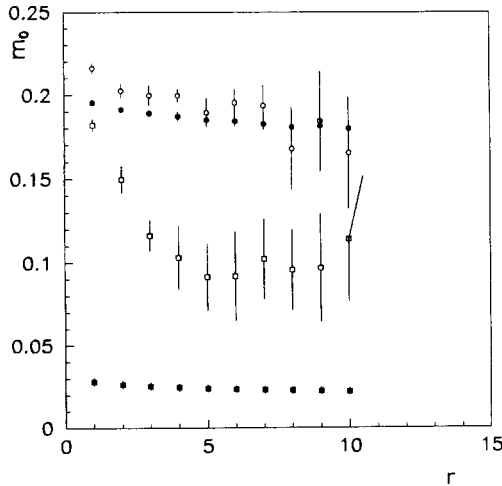


Fig. 11. Distance-dependent masses obtained from  $R_0^\alpha$  (full symbols) and  $R_0^\beta$  (open symbols) for  $L = 36$  and  $\beta = 0.365$  (dots) and  $\beta = 0.367$  (squares).

TABLE 5  
 $m_1^\beta$  for all values of  $\beta$  and lattices of sizes  $L = 20, 24, 30, 36$  and  $48$  obtained from fits to the correlation functions  $\Gamma_1^{\text{diff}}(r)$ . Fits for  $L \geq 24$  have been performed for  $r \geq 6$ , while those for  $L = 20$  are based on all  $r \geq 4$

$\beta \backslash L$	20	24	30	36	48
0.365	0.224(1)	0.202(5)	0.194(2)	0.196(2)	0.193(2)
0.3655	0.210(3)	0.181(3)	0.180(2)	0.180(9)	0.179(3)
0.366	0.190(2)	0.159(4)	0.161(2)	0.164(9)	0.158(4)
0.3665	0.186(6)	0.134(7)	0.128(2)	0.136(1)	0.142(5)
0.36675	0.175(10)	0.144(9)	0.124(4)	0.118(3)	0.124(3)
0.36689	—	—	—	0.114(6)	0.107(7)
0.367	0.196(7)	0.153(15)	0.126(5)	0.115(7)	0.099(12)
0.367025	—	—	—	—	0.112(24)
0.36705	—	—	—	—	0.112(19)
0.3671	—	—	—	—	0.134(8)
0.36715	—	—	—	0.131(13)	0.142(7)
0.36725	0.207(11)	0.171(13)	0.171(11)	0.152(5)	0.165(9)
0.3675	0.231(7)	0.193(10)	0.201(5)	0.193(3)	0.194(6)
0.368	0.280(3)	—	0.249(2)	0.253(4)	0.241(6)

correlation function  $\Gamma^{\text{diff}}$  will be dominated by the next higher mass scale. We further note that finite size effects in these estimates seem to be considerably smaller close to  $\beta_c$  than those based on unsubtracted correlation functions. In particular,  $1/m^\beta$  does not scale as  $L$  at  $\beta \sim 0.367$ .

Summarizing the results of this section in brief, we find that a study of correlation lengths alone is inadequate to determine the order of the phase transition in the 3-d three-state Potts model. The primary reason behind this is that various methods to extract correlation lengths from data on finite lattices do not agree in the critical region, although they do so sufficiently far away from  $\beta_c$ . While the estimates of correlation lengths obtained from the ratios  $R_i^\alpha$  suggest  $\xi \sim L$  at  $\beta_c$ , a finite correlation length ( $\xi \simeq 10$ ) is indicated by the ratios  $R_i^\beta$ . The former is related to the tunnelling correlation length whereas the latter yields the inverse mass gap in the infinite volume limit.

#### 4. Conclusions

Motivated by the recent controversy about the order of the phase transition in finite temperature SU(3) gauge theory and its consequent impact on the universality picture, we have investigated the 3-d three-state Potts model on lattices of size  $L^3$  for  $L = 12, 20, 24, 30, 36$  and  $48$  in a high statistics Monte Carlo simulation. The analysis of global quantities like energy density and order parameter re-establishes clearly the first-order nature of the phase transition in the Potts model. The finite size corrections to the critical coupling and the width of the metastable region are

consistent with the  $1/V$  behaviour expected for a first-order phase transition. The probability distribution for the order parameter shows a distinct two-peak structure. The location of the peaks is rather insensitive to the lattice size and the overlap of their tails decreases with increasing  $L$ . This gives rise to a finite gap in the order parameter as well as in the action. The characteristics of the transition in the infinite volume limit, obtained by two different extrapolation methods, are

$$\begin{aligned}\beta_c &= 0.36708 \pm 0.00002, \\ \Delta S &= 0.395 \pm 0.005, \\ \Delta E &= 0.080 \pm 0.004.\end{aligned}\tag{4.1}$$

We also calculated spin-spin correlation functions ( $\Gamma_1$ ) and the corresponding zero-momentum plane-plane correlations ( $\Gamma_0$ ). Various known methods were used to extract the correlation lengths from these observables. In general, the results obtained from  $\Gamma_0$  and  $\Gamma_1$  agreed with each other, although for  $\xi \geq 10$  we needed a generalized periodic exponential that incorporated the periodicity in transverse directions. The different methods used to extract  $\xi$  yielded the same results only away from the critical region. Approaching the critical region one found that the masses estimated from the ratios of plain correlation functions,  $R^\alpha$ , decreased monotonically across  $\beta_c$  whereas those obtained from the ratios of differences of correlation functions,  $R^\beta$ , had a minimum at  $\beta_c$ . On a finite lattice it is expected that one more correlation length besides the inverse mass gap, the tunnelling correlation length, becomes relevant especially for  $\beta \geq \beta_c$ . Since the tunnelling correlation length is infinite in the entire range of  $\beta \geq \beta_c$  for an infinite lattice it is natural to expect that on finite lattices it is the largest one in that domain. Consequently the latter set of ratios is better suited to obtain the inverse mass gap in the critical region. Based on this, we find that the inverse mass gap stays finite at  $\beta_c$ ,

$$\xi(\beta_c) \sim 10.\tag{4.2}$$

Our final results on the mass gap in the 3-d three-state Potts model obtained on the largest lattice analysed are given in fig. 12.

Let us finally discuss the relevance of our results for the SU(3) deconfinement phase transition. Our observation of a clear signal for a first-order phase transition in global observables is in qualitative agreement with the corresponding findings for the SU(3) order parameter and internal energy [9]. Also as in the case of SU(3) [8], the ratios  $R_i^\alpha$  yield in our case a correlation length that diverges with the length of the system at  $\beta_c$ . However, we do not expect this to reflect the true behaviour of the physical mass gap in the infinite volume limit due to the inevitable mixing between the tunnelling correlation length and the inverse mass gap on finite lattices.

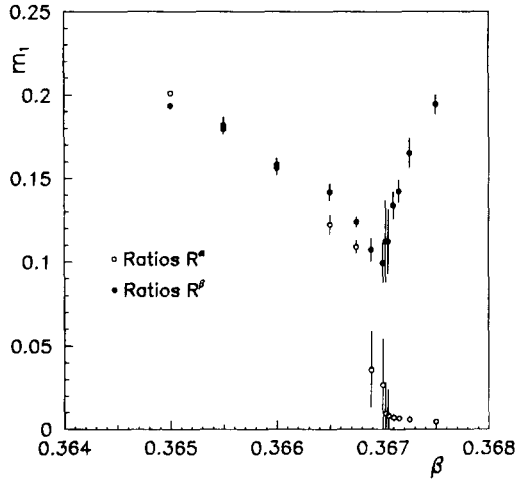


Fig. 12.  $m_1^a$  and  $m_1^b$  as a function of  $\beta$  for the  $48^3$  lattice.

In the case of the 3-d three-state Potts model the estimate of the correlation length based on differences of the correlation functions seems to be a better indicator of the infinite volume correlation length on finite lattices, despite the fact that it is more difficult to obtain it with high accuracy. This correlation length stays finite at  $\beta_c$  and shows only little size dependence when we change the lattice size from  $L = 30$  up to  $L = 48$ . Also in the case of  $SU(3)$  gauge theory it may therefore be useful to extract the correlation length from the ratios  $R_i^\beta$  in the critical region. If it turns out that the correlation length obtained even from this ratio increases with the size of the system, then it would indeed be a remarkable difference compared to the behaviour of the Potts model and would cast doubts on the standard universality arguments in the case of a global  $Z(3)$  symmetry.

To be sure, the results of ref. [8] are not comparable directly with ours because of the different geometry and boundary conditions of the lattice employed by us. Whereas we use a cubic lattice with periodic boundary conditions, ref. [8] used a cylindrical geometry with a cold wall at the ends of the cylinder. We are presently investigating the relevance of these differences for the conclusions reached above.

## References

- [1] L.G. Yaffe and B. Svetitsky, Phys. Rev. D26 (1982) 963
- [2] H.W.J. Blöte and R.H. Swendsen, Phys. Rev. Lett. 43 (1979) 799
- [3] S.J. Knak Jensen and O.J. Mouritsen, Phys. Rev. Lett. 43 (1979) 1736
- [4] F.Y. Wu, Rev. Mod. Phys. 54 (1982) 235
- [5] J. Kogut, et al., Phys. Rev. Lett. 51 (1983) 869;  
T. Celik, J. Engels and H. Satz, Phys. Lett. B129 (1983) 323.
- [6] A. Kennedy et al., Phys. Rev. Lett. 54 (1985) 87

- [7] N. Christ and A.E. Terrano, *Phys. Rev. Lett.* 56 (1986) 111
- [8] P. Bacilieri et al., *Phys. Rev. Lett.* 61 (1988) 1545
- [9] F.R. Brown, N.H. Christ, Y. Deng, M. Gao and T.J. Woch, *Phys. Rev. Lett.* 61 (1988) 2058
- [10] M.N. Barber, *in* Phase transitions and critical phenomena, Vol. 8, ed. C. Domb and J.L. Lebowitz (Academic Press, New York, 1983) p. 145
- [11] M.E. Fisher and A.N. Berker, *Phys. Rev.* B26 (1982) 2507
- [12] H.W.J. Blöte and M.P. Nightingale, *Physica* 112A (1982) 405
- [13] V. Privman and M.E. Fisher, *J. Stat. Phys.* 33 (1983) 385
- [14] M. Lüscher, *Nucl. Phys.* B219 (1983) 233
- [15] E. Brezin and J. Zinn-Justin, *Nucl. Phys.* B257 [FS14] (1985) 867
- [16] B.A. Berg, A. Billoire and R. Salvador, *Phys. Rev.* D37 (1988) 3774
- [17] T.D. Schultz, D.C. Mattis and E.H. Lieb, *Rev. Mod. Phys.* 36 (1964) 856
- [18] K. Jansen et al., Vacuum tunnelling in the 4-dimensional Ising model, DESY 88-096, July 1988
- [19] I. Montvay and P. Weisz, *Nucl. Phys.* B290 [FS20] (1987) 327